Analysis of Paper-Based Colorimetric Assays With a Smartphone Spectrometer

Elizabeth V. Woodburn, Kenneth D. Long, and Brian T. Cunningham, *Fellow, IEEE*

***Abstract*— We report on the adaptation of a smartphone's rear-facing camera to function as a spectrometer that measures the spectrum of light scattered by common paper-based assay test strips. We utilize a cartridge that enables a linear series of test pads in a single strip to be swiped past the read head of the instrument while the phone's camera records video. The strip is housed in a custom-fabricated cartridge that slides through the instrument to facilitate illumination with white light from the smartphone's flash LED that is directed through an optical fiber. We demonstrate the ability to detect subtle changes in the scattered spectrum that enables quantitative analysis of single-analyte and multi-analyte strips. The demonstrated capability can be applied to broad classes of paper-based assays in which visual observation of colored strips is not sufficiently quantitative, and for which analysis of red-green-blue pixel values of a camera image are not capable of measuring complex scattered spectra.**

***Index Terms*— Biomarkers, biomedical monitoring, biosensors, cellular phones, multimodal sensors, patient monitoring, point-of-care, smartphone biosensing, smartphone spectroscopy.**

I. Introduction

ASSAYS that generate a colored liquid or a fluorescence-generating liquid represent broad classes of tests that are used in many applications that include health and wellness diagnostics [1], water and food safety monitoring [2], manufacturing quality control [3], forensic analysis, and product authenticity verification [4]. For these applications, the ability to measure the visible-wavelength absorption/emission spectrum not only enables the system to be applicable to a broad range of chromophores and fluorophores, but also facilitates the quantification of subtle changes in color that are not possible to differentiate by analyzing small set of wavelengths (such as with a few color filters, or through analysis of the red-green-blue pixel intensities of a conventional image).

In this work, we demonstrate quantitative smartphone-based spectral analysis of a further broad and commercially important class of assays: paper test strips. Paper-based test strips have been commercially available for many years [5] for applications that include fundamental characteristics of liquids (pH, alkalinity, chlorine), lateral flow assays for health conditions (i.e. pregnancy) or diseases [6], and blood analysis [7]–[9]. Most typically, the color of a test strip is analyzed by visual comparison against a set of color standards, to roughly estimate the concentration of the target analyte. However, subtle color variations can be difficult to differentiate, with variability induced by factors that include the observational powers of individual users and lighting conditions. The chromophores produced by paper test strips vary widely across the palette, with complex spectra that incorporate many wavelength components that combine to produce the observed color. Spectroscopic analysis of the scattered light spectrum from paper test strips reveals subtle features that are not visually quantifiable, and that can be used to provide more precise information. As a representative example, here we focus on measuring the scattered light spectrum from paper test strips used for urine analysis.

Urine dipsticks have been used as a point-of-care (POC) diagnostic test since the introduction of Clinistix glucose urinalysis strips in 1956 [5]. When the dry reagent pad is dipped into a urine sample, a color change proportional to the amount of glucose in the urine occurs and can be compared to a color chart in order to obtain semi-quantitative results. Further advancements in dry reagent pad tests have yielded widely-used commercial products in which a standard panel tests for ten analytes on a single strip. Bayer Multistix 10 SG represents an early version of this test, introduced in 1984 to test for glucose (GLU), protein (PRO), ketones (KET), pH, blood (BLO), bilirubin (BIL), urobilinogen (URO), nitrite (NIT), specific gravity (SG), and leukocytes (LEU). Whereas dipsticks are used in POC diagnostics on a variety of animals, we choose here to focus on a human application [10]–[12].

Urine tests are a standard part of diabetic self-monitoring for the presence of ketones, where detection of low levels can aid in early detection and management of diabetic ketoacidosis (DKA) [13]. Self-tests for the presence of urinary protein have been shown to serve as an effective screening tool for kidney damage [14], [15]. Dipsticks are also used in the clinical setting, where positive values for leukocytes, nitrite, blood, and protein may indicate the presence of a urinary tract

Manuscript received July 20, 2018; revised October 9, 2018; accepted October 11, 2018. Date of publication October 17, 2018; date of current version December 21, 2018. This work was supported in part by the National Science Foundation under Grant CBET 12-64377 and in part by the National Institutes of Health under Grant F30AI122925. The associate editor coordinating the review of this paper and approving it for publication was Dr. Ioannis Raptis. *(Corresponding author: Brian T. Cunningham.)*

E. V. Woodburn was with the Department of Bioengineering, University of Illinois at Urbana–Champaign, Urbana, IL 61801 USA. She is now with the Carle Illinois College of Medicine, Champaign, IL 61820 USA (e-mail: woodbrn2@illinois.edu).

K. D. Long is with the Department of Bioengineering, University of Illinois at Urbana–Champaign and the College of Medicine, University of Illinois at Urbana–Champaign, Urbana, IL 61801 USA (e-mail: long6@illinois.edu).

B. T. Cunningham is with the Department of Electrical and Computer Engineering and the Department of Bioengineering, University of Illinois at Urbana–Champaign, Urbana, IL 61801 USA (e-mail: bcunning@illinois.edu).

This paper has supplementary downloadable multimedia material available at http://ieeexplore.ieee.org provided by the authors. The Supplementary Material contains additional figures demonstrating results from different tests of measurement variation, as referenced within the main article. This material is 134 KB in size.

Digital Object Identifier 10.1109/JSEN.2018.2876631

infection (UTI). Increased usage of dipsticks has been shown to reduce the need to send specimens into laboratories for full urinalysis, allowing patients to receive results quickly and at a reduced cost to the healthcare system [16]–[18].

Whereas dipsticks are designed to be read by visual analysis, automated analyzers have been shown to reduce variation and error in test results [19]–[21]. When considering the further comorbidity between diabetes and visual impairment, visual analysis increases the likelihood of improper test interpretation [22], [23]. Semi-quantitative reflectance photometry has thus been maintained as the gold standard for automated POC urinalysis, with multi wavelength measurement devices becoming more common [21], [24], [25]. However, commercially available automated urinalysis dipstick analyzers are expensive, and usually compatible only with specific dipstick brands. To address these issues, several different approaches to automated smartphone analysis of urine strips have been proposed, all reliant on comparing photos taken of the strips when wet to color charts [26]–[29]. While portable and inexpensive when compared to commercial analyzers, these devices are still limited to a single biosensing modality and have limited functionality compared to full spectroscopic analysis systems.

Recently, we demonstrated a compact "cradle" for an ordinary smartphone that enabled its rear-facing camera to be utilized as a spectrophotometer for measuring the absorption spectra of bio-assay liquids [2], the fluorescence emission spectra from tagged nucleic acids [30], and the resonant reflection spectra from label-free photonic crystal biosensors. The Transmission-Reflection-Intensity (TRI)-Analyzer is capable of utilizing the rear-facing flash LED to channel broadband "white" light to a test sample through an optical fiber, and to gather light from a test sample into a separate optical fiber that directs light through a diffraction grating placed directly in front of the camera lens [1]. The cradle, comprised of a plastic housing that places inexpensive passive optical components into alignment with the LED and camera of a mobile phone, was demonstrated to perform an equivalent function to laboratory-based spectrophotometers in terms of detection limit and dynamic range for several representative assays [1]. Although the read head of the instrument illuminates only a single point, we also demonstrated that a cartridge comprised of a linear series of liquid compartments could be measured rapidly in series by scanning the cartridge through the instrument while the phone's camera records video, using an image processing algorithm to automate selection of video frames that represent spectra from the center of each compartment. By performing data capture and image processing with the smartphone's internal microprocessor, resulting data can be easily shared with cloud-based service systems such as those used by healthcare providers, epidemiology, and quality control [31].

In this work, we demonstrate the additional ability of the spectral TRI-analyzer to quantitatively analyze color changes produced by multiple analytes on POC urinalysis strips. The user dips the strip into a urine sample and removes excess liquid before placing it into a low-cost disposable cartridge. After the strip has been allowed to dry, the cartridge is then manually swiped through the cradle for analysis of light scattered by each sample pad. We demonstrate the ability to differentiate between clinically significant high and low values of 10 different analytes in urine samples, as well as the ability to quantify low concentrations of ketones and glucose.

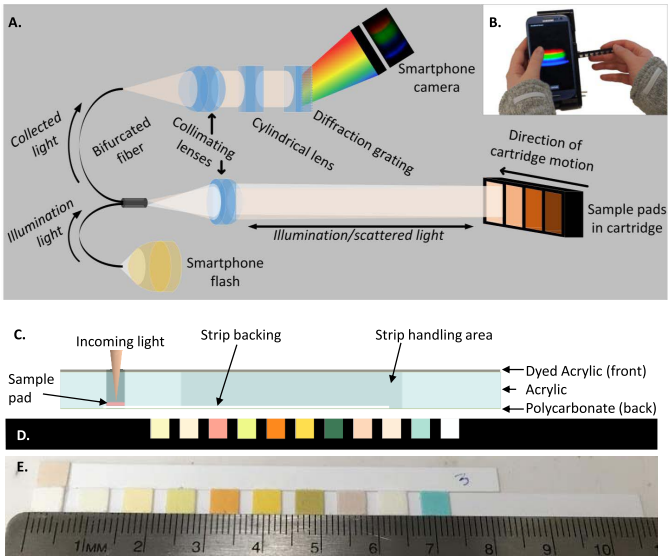

Fig. 1. Cradle and cartridge designs along with principal light path. (A) The bifurcated optical fiber allows for usage of the smartphone flash and camera for sample illumination and detection pathways. Focused light from the smartphone flash LED illuminates the sample pads as they move across the light path, and scattered light is collected for delivery to the camera. (B) Demonstration of sample cartridge being manually inserted into the cradle. (C) Top-down view of the ketone strip in its cartridge. Layers of acrylic, double-sided adhesive (DSA), and polycarbonate film are laser-cut and assembled to facilitate usage of different strip layouts. (D) Front view of the 10-reagent strip in its cartridge. The extra opening at the end allows for usage of the white backing as a reference surface. Dividers between samples are dyed black in order to clearly separate the samples in the raw video collected of each swipe. (E) Ketone and 10-reagent strips pictured with ruler for scale. Adapted from *Food Chemistry, 272*, M. A. Aguirre, K. D. Long, A. Canals, and B. T. Cunningham, "Point-of-use detection of ascorbic acid using a spectrometric smartphone-based system," 141-147, Copyright 2018, with permission from Elsevier.

II. Methods

A. Smartphone Cradle Construction

The TRI-Analyzer is comprised of a smartphone with a custom-fabricated cradle that allows the phone's rear-facing camera to act as a spectrometer. The scattering modality utilizes the light path originally created for quantifying absorption of liquid samples, with the addition of an extra lens to efficiently gather scattered photons from the illuminated test strip surface (Fig. 1(A)). White light from the phone's LED flash is collected by one arm of a bifurcated multimodal optical fiber (d = 200μm), which transmits through two planoconvex (PCX) lenses that focus the incident light to a point on the test strip surface. Scattered light is then collected via the other arm of the bifurcated fiber and transmitted through achromatic and cylindrical lenses that collimate and focus it in the non-spectral dimension through the aperture of the smartphone camera. A diffraction grating placed directly over the camera diffracts the light in the spectral dimension, producing a wavelength-resolvable image.

The cradle was fabricated using a stereolithography-based 3D printer (Formlabs) to hold the optical components to align with the locations of the flash LED and the image sensor for the smartphone (Samsung, Galaxy S3). A copper spring holds the cartridge against the rear wall of the instrument's cartridge slot, to ensure that the test strip surface is in a consistent plane with respect to the tip of the optical fiber illuminate/read head. The cost of components is approximately $550, when purchased as individual units. As discussed previously, utilizing optical fibers and a 3D printed cradle to align the light path allows the system to be reconfigured with relative ease to interface with different smartphones [1].

B. Sample Cartridge Construction

A cartridge design was developed utilizing layers of laser-cut acrylic of varying thickness, double-sided adhesive (DSA; 3M, #8212), and polycarbonate film to allow samples to interface with the cradle. Ketone strip cartridges were composed of (1) a 1/32" acrylic top layer, (2) a 3/8" acrylic cavity layer, and (3) a polycarbonate film backing, all adhered with DSA layers (Fig. 1(C)). Multi-reagent strip cartridges were composed of (1) a 3/8" acrylic top layer and (2) a polycarbonate film backing, adhered with a single layer of DSA (Fig. 1(D)). The front layer in each cartridge was coated with opaque black dye (Dykem 81724) in order to provide high contrast between wells for the video frame analysis algorithm. Strips can be inserted and pushed through by hand in a user-friendly manner that protects the sample pad surface and prevents liquids from contaminating the cradle.

C. Data Collection and Analysis

When collecting data from 10-analyte strips, the cartridge is moved through the cradle with a swiping motion while a video sequence of images is taken at a rate of 60 frames/sec. The black dividers between each sample well produce significant troughs in average pixel intensity value from frame to frame that can be used to differentiate the boundaries between each of the 10 samples. The frames (each frame represents a scattered spectrum) for each sample are then averaged into a single image; this process helps to correct for any uneven color distribution present within a single sample pad. Spectral profiles were then obtained using average pixel values from three sequential swipes of each strip. When collecting data from single-analyte strips, the cartridge is inserted into the cradle before several pictures are taken of a single location on the sample pad. Multiple frames or pictures, respectively, are then averaged for further analysis.

A "mask" overlay is obtained by taking a picture of a mirror, converting it to grayscale, and excluding pixels with an intensity below 240. This ensures that any pixels outside the maximum range obtainable by the device are excluded. A plot of the spectrum is generated by capturing images of red and green laser pointers and finding the pixel index of their respective peaks. By measuring the same laser pointers on a benchtop spectrometer, spectral images can be converted to spectral plots measured in units of nanometers wavelength. Pixel resolution of the device in photo mode was calculated using the laser ($\Delta\lambda$ = 124.16 nm)/(n = 410.17 pixels) = 0.3027 nm/pixel.

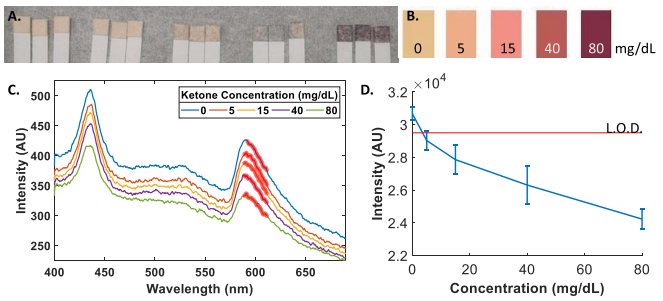

Fig. 2. Demonstration of ketone detection. (A) Dried strips are shown in order of increasing solution concentration from 0 to 80 mg/dL, three strips per solution. (B) The provided color chart used to manually read the strips when wet. (C) Spectral data obtained as the average of the three strips at each concentration. The analysis wavelengths between 589-612 nm is highlighted. (D) Dose-response curve generated using area under the curve (AUC) value for the designated region. Plotted values show the mean value of the three strips, with error bars representing standard deviation (SD). The horizontal line represents the limit of detection (LOD), chosen as three times the SD of the 0 mg/dL concentration, of 3.5 mg/dL.

III. Results and Discussion

A. Device Characterization

The cell phone camera includes pre-set white balance options, designed to adjust for the ambient lighting "temperature." Spectra were obtained for paper samples that were tan, red, green, blue, and white under four separate white balance settings on the smartphone. The "cloudy" setting was chosen for use in all further experiments due to its ability to generate the highest overall intensity, and to best differentiate between the five measured colors. The wavelength range of 589-612 nm was identified as having the greatest degree of separation between individual colors, and thus its area under the curve (AUC) value was used for single-analyte strip measurements.

Spectra were obtained for individual and sequential pictures of a single piece of white paper without removing it from the device to determine the noise level of the device itself. When averaging the target AUC for three individual pictures, the standard deviation was only 0.29% of the mean value (Fig. S1(a)). When inserting the same white paper 5 times and evaluating the AUC across the target area, standard deviation was only 0.97% of the mean value (Fig. S1(b)).

When looking at six dry ketone strips evaluated individually, standard deviation is 1.01% of the mean value; this suggests that some of the variation visible between trials may be due to variation in the strips themselves, rather than the device or user error (Fig. S1(c)). A single ketone strip was then loaded with deionized water and placed in the cradle to dry, with measurements taken at 15 second intervals (Fig. S1(d)). Although the strips are intended to be evaluated 15 seconds after dipping in urine, the sample evaporation that occurs during this interval has a large effect on the accuracy and repeatability of the measurement. Therefore, all measurements were taken from strips allowed to dry at room temperature

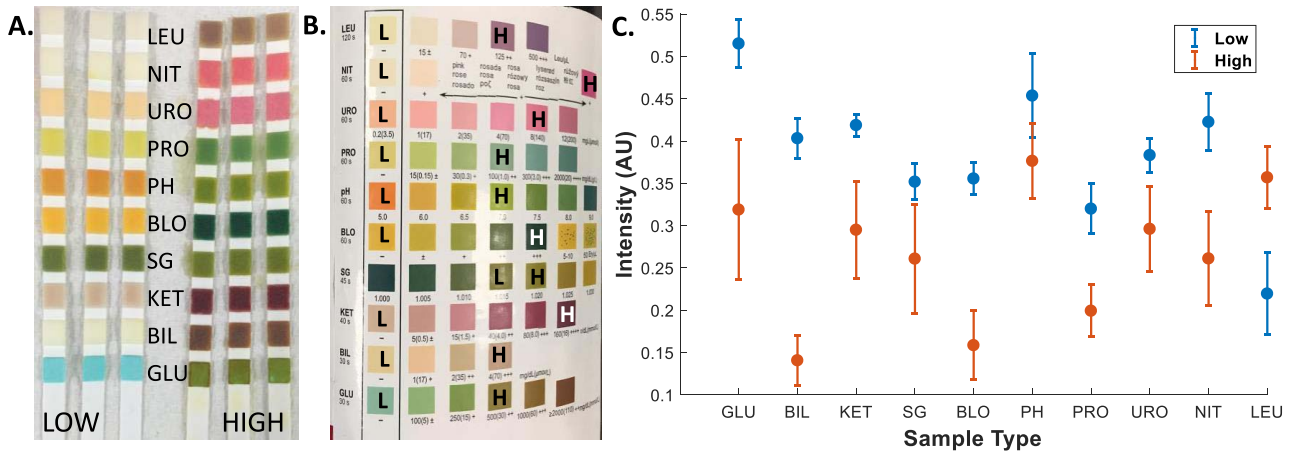

Fig. 3. Demonstration of differentiation between high and low sample concentrations. (A) Strips shown immediately after having been dipped in calibration solutions containing low (L) and high (H) concentrations of each analyte. (B) The provided color chart used to manually read the strips when wet. Low (L) and high (H) values are shown over their respective reading value. (C) Values obtained for each of the 10 analytes, shown as the mean of three strips with standard deviation. Readings were taken when the strips were dry to minimize evaporation-based variation.

for 40 minutes after sample application in order to minimize variability in scattered spectra that occurs during evaporation.

B. Ketone Dose-Response Characterization

To validate the ability of the device to distinguish between solutions of a urine analyte at various clinically relevant concentrations, single-reagent ketone dipsticks (Bayer Ketostix) were used to detect the most common urinary ketone of acetoacetic acid. Serial dilutions of lithium acetoacetate (Sigma Aldrich) in water were prepared at concentrations of 0, 5, 15, 40, and 80 mg/dL to match the reference color ranges provided to read the strips (Fig. 2(B)). Three strips were dipped into each of the concentrations and evaluated for scattering in the TRI-Analyzer after drying (Fig. 2(A)).

A dose-response curve was created using AUC values for the 589-612 nm wavelength range (Fig. 2(C)), along with standard deviation for each of the three trials (Fig. 2(D)). The Limit of Detection (LOD) was estimated to be approximately 3.5 mg/dL, which is lower than the 5 mg/dL LOD for human visual analysis via color chart comparison. Of the two most common types of ketone bodies that appear in human urine, β-hydroxybutyrate appears earliest in DKA, but urinalysis strips are most sensitive to acetoacetic acid [32]. Thus, it is desirable to be able to consistently identify low urinary concentrations of acetoacetic acid in order to detect early DKA. While diagnostic criteria for DKA include ketone concentrations greater than 17 mg/dL, concentrations above 3.5 mg/dL indicate abnormal levels of ketone production [22].

C. Multi-Reagent Detection

Multi-reagent strips measure nine analytes in addition to ketones, but each of the 10 sample pads is intended to be read at a designated time after sample application ranging from 15 to 120 seconds. To validate the ability of the TRI-Analyzer to differentiate between high and low concentrations at an analysis time of 40 minutes, human urine-based controls (Kova) representing normal and abnormal analyte concentrations were reconstituted in water. Three strips (MooreBrand Urine Reagent Strips 10 SG) were dipped into each of the concentrations and their color changes within the target reading time of 30 to 120 seconds (Fig. 3(A)) were compared to the provided color chart (Fig. 3(B)) in order to estimate the relative concentrations of each analyte. After drying, the strips were evaluated in the cradle and spectral profiles obtained. AUC values for analyte-specific regions were averaged across the three strips (Fig. 3(C)).

Separation of mean values at each concentration for all analytes except specific gravity and pH were found to be statistically significant ($p < 0.05$) using an unpaired two-sample t-test. Visible overlap in pH readings results from usage of a dual-indicator test that is not compatible with quantification via single-region spectral analysis. Whereas SG values obtained from the TRI-Analyzer show little separation when looking at variation, the values obtained from the color chart of 1.015 and 1.020 are adjacent. In comparing the wet samples to the color chart, it can be noted that hues are often difficult to match precisely to individual color blocks; therefore, spectral analysis may be useful for obtaining quantitative measurements without risking the involvement of human visual inter-rater reliability.

D. pH Dose-Response Characterization

A calibration curve was created for pH measurements ranging from 6.0 to 8.4 (Fig. 4(e)). Solutions were created by adding $NaHCO_3$ to the normal urine control solution in order to raise the pH from its starting value of 6.0, as evaluated on a benchtop pH meter (Thermo, Orion 4-Star). Three strips were dipped into each of the solutions and their color changes at the target reading time of 60 seconds (Fig. 4(A)) were compared to the provided color chart (Fig. 4(C)). After drying, the strips were evaluated in the TRI-Analyzer and spectral profiles obtained and plotted as the mean of the three strips (Fig. 4(D)).

Since the pH detection pads make use of a dual-indicator system, two spectral regions were used in order to create the calibration curve. Methyl red has an active range of

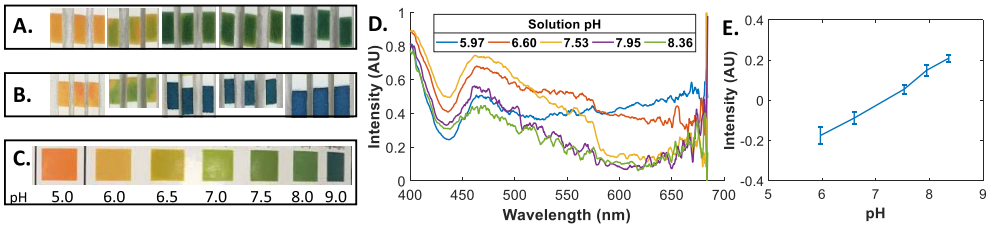

Fig. 4. Demonstration of pH detection. (A) Wet strips are shown in order of increasing solution pH from 6.0 to 8.4, three strips per solution. (B) Same strips shown at time of measurement, after 40 minutes of drying. (C) The provided color chart used to manually read the strips when wet. (D) Spectra data obtained as the average of the three strips at each concentration. (E) Detection curve calculated using AUC values for the wavelengths between 460 -470 and 630-640 nm. Plotted values show the mean value of the three strips, with error bars representing SD for each calculation.

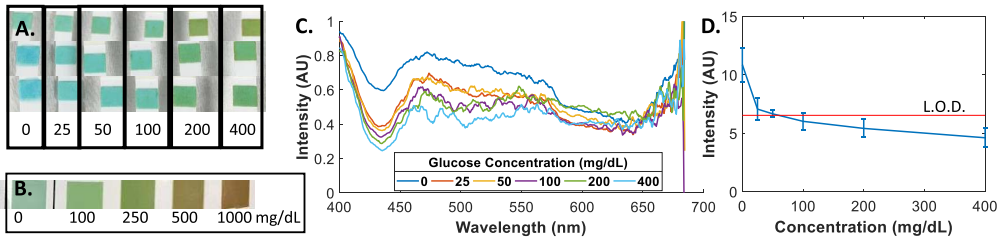

Fig. 5. Demonstration of glucose detection. (A) Dried strips are shown in order of increasing solution concentration from 0 to 400 mg/dL, three strips per solution. (B) The provided color chart used to manually read the strips when wet, with values ranging from 0-1000 mg/dL. (C) Spectral data obtained as the average of the three strips at each concentration. The wavelengths between 430-440 nm were used for analysis. (D) Dose-response curve generated using AUC value for the designated region. Plotted values show the mean value of the three strips, with error bars representing standard deviation (SD). The horizontal line represents the LOD, chosen as three times the SD of the 0 mg/dL concentration, of 60 mg/dL.

pH 4.4 to 6.2. Bromothymol blue has a pH indicator active range of 6.0 to 7.6, with blue appearing much more strongly in basic solutions. Continued blue color development as the strips dried made pH values of 7.5 to 8.4 visually indistinguishable (Fig. 4(B)) but produced a significant decrease in measured scattering at wavelengths in the red spectral region. As such, AUC values for the 630-640 nm wavelength range were used only for analysis of solutions with pH greater than 7. AUC values using the 460-470 nm wavelength range were used for analysis of all solutions. The ability to differentiate between readings that visually appear nearly identical demonstrates the value of spectral analysis, rather than simple evaluation of color photographs.

E. Glucose Dose-Response Characterization

After demonstrating the ability of the device to distinguish between high and low analyte concentrations, glucose was chosen for further quantitative study. Serial dilutions of glucose in normal control urine solution were prepared at concentrations of 0, 25, 50, 100, 200, and 400 mg/dL. Since the glucose concentration of the original control solution was known only to be under 100 mg/dL, these concentrations represent only the known added amount of glucose. Three strips were dipped into each of the concentrations, and their color changes at 15 seconds after sample application (Fig. 5(A)) visually compared to the provided color chart (Fig. 5(B)). After drying, the strips were evaluated in the TRI-Analyzer and spectral profiles obtained and plotted as the mean of the three strips at each concentration (Fig. 5(C)).

A dose-response curve was created using mean AUC values for the 430-440 nm wavelength range along with standard deviation for each of the three trials (Fig. 5(D)). The LOD was estimated to be approximately 60 mg/dL, which is lower than the 100 mg/dL LOD for human visual analysis via color chart comparison. While the sensitivity of the device is low in the upper range of physiologic glucose concentrations, we believe that the inherently adaptable device design will allow future iterations to collect a stronger signal and obtain levels of sensitivity more suitable for intensive patient glucose management. The TRI-Analyzer was constructed for use with three other principal light paths, none of which require as much incident light as scattering. Future iterations will be able to take advantage of the significant progress made in low-light smartphone camera hardware since 2013, as well as possibly integrate a more efficient collection interface with the smartphone flash.

IV. Conclusion

While POC urine dipsticks are inexpensive and user-friendly by nature, the ability to read them with digital analyzers improves both inter-rater and intra-rater reliability. By utilizing the inherent connectivity features of smartphones, results can be easily stored, compared, and sent to clinicians for further interpretation. When incorporated into a multimodal device, such as the TRI-Analyzer, which is also capable of reading the output of liquid based colorimetric and fluorescent assays, patient and clinicians gain access to a POC laboratory system that can be used for an enormous variety of diagnostic and monitoring tests.

In this work, we demonstrated the ability of the multimodal TRI-Analyzer system to differentiate between color changes generated by various analytes on urinalysis strips. While a healthy human eye can tell rudimentary colors apart, it does not possess the resolution of a spectrometer or its ability

for wavelength-specific analysis and de-coupling of combined colors. Spectral analysis may also open the door for usage of different color indicators in diagnostic test strips that may not be resolvable by the human eye but have a broader dynamic range or greater sensitivity.

Demonstrating the ability of the TRI-Analyzer to evaluate solid samples, in addition to the liquids used in previous modalities, further broadens the scope of diagnostic tests that it is compatible with. Owing to its customizable design, we anticipate that future improvements in smartphone camera technologies will continue to strengthen its ability to increase access to quality point-of-care diagnostics.

ACKNOWLEDGMENT

The authors thank the Illinois Scholars Undergraduate Research Program for supporting this project.

REFERENCES

[1] K. D. Long, E. V. Woodburn, H. M. Le, U. K. Shah, S. S. Lumetta, and B. T. Cunningham, "Multimode smartphone biosensing: the transmission, reflection, and intensity spectral (TRI)-analyzer," *Lab Chip*, vol. 17, no. 19, pp. 3246–3257, Jul. 2017.

[2] K. D. Long, H. Yu, and B. T. Cunningham, "Smartphon instrument for portable enzyme-linked immunosorbent assays," *Biomed. Opt. Express*, vol. 5, no. 11, pp. 3792–3806, Nov. 2014.

[3] M. A. Aguirre, K. D. Long, A. Canals, and B. T. Cunningham, "Point-of-use detection of ascorbic acid using a spectrometric smartphone-based system," *Food Chem.*, vol. 272, pp. 141–147, Jan. 2019.

[4] H. Yu *et al.*, "Characterization of drug authenticity using thin layer chromatography imaging with a mobile phone," *J. Pharm. Biomed. Anal.*, vol. 125, pp. 85–93, Jun. 2016.

[5] M. J. Pugia, "Technology behind diagnostic reagent strips," *Lab. Med.*, vol. 31, no. 2, pp. 92–96, Feb. 2000.

[6] K. M. Koczula and A. Gallotta, "Lateral flow assays," *Essays Biochem.*, vol. 60, no. 1, pp. 111–120, Jun. 2016.

[7] Y. Harano, M. Suzuki, H. Kojima, A. Kashiwagi, H. Hidaka, and Y. Shigeta, "Development of paper-strip test for 3-hydroxybutyrate and its clinical application," *Diabetes Care*, vol. 7, no. 5, pp. 481–485, Sep./Oct. 1984.

[8] R. D. Cheeley and S. M. Joyce, "A clinical comparison of the performance of four blood glucose reagent strips," *Am. J. Emerg. Med.*, vol. 8, no. 1, pp. 11–15, Jan. 1990.

[9] J. Tenuovo and T. Anttonen, "Application of a dehydrated test strip, HEMASTIX, for the assessment of gingivitis," *J. Clin. Peridontol.*, vol. 5, no. 3, pp. 206–212, Aug. 1978.

[10] J. Carrier, S. Stewart, S. Godden, J. Fetrow, and P. Rapnicki, "Evaluation and use of three cowside tests for detection of subclinical ketosis in early postpartum cows," *J. Dairy Sci.*, vol. 87, no. 11, pp. 3725–3735, Nov. 2004.

[11] M. Defontis, N. Bauer, K. Failing, and A. Moritz, "Automated and visual analysis of commercial urinary dipsticks in dogs, cats and cattle," *Res. Vet. Sci.*, vol. 94, no. 3, pp. 440–445, Jan. 2013.

[12] C. J. Savage, "Urinary clinical pathologic findings and glomerular filtration rate in the horse," *Vet. Clin. North Am. Equine Pract.*, vol. 24, no. 2, pp. 387–404, Aug. 2008.

[13] National Clinical Guideline Centre, "Ketone monitoring and management of diabetic ketoacidosis (DKA)," in *Type 1 Diabetes in Adults: Diagnosis and Management*. London, U.K.: National Institute for Health and Care Excellence, 2015.

[14] M. M. Nielen, F. G. Schellevis, and R. A. Verheij, "The usefulness of a free self-test for screening albuminuria in the general population: A cross-sectional survey,"*BMC Public Health*, vol. 9, p. 381, Oct. 2009.

[15] A. Heidland, *et al.*, "Mass-screening for early detection of renal disease: Benefits and limitations of self-testing for proteinuria," *J. Nephrol.*, vol. 22, no. 2, pp. 249–254, Mar. 2009.

[16] H. Patel, "Can urine dipstick testing for urinary tract infection at point of care reduce laboratory workload?" *J. Clin. Pathol.*, vol. 58, no. 9, pp. 951–954, Sep. 2005.

[17] C. Hiscoke, H. Yoxall, D. Grieg, and N. F. Lightfoot, "Validation of a method for the rapid diagnosis of urinary tract infection suitable for use in general practice," *Br. J. Gen. Pract.*, vol. 40, no. 339, pp. 403–405, Oct. 1990.

[18] A. Malmartel, M. Dutron, and C. Ghasarossian, "Tracking unnecessary negative urinalyses to reduce healthcare costs: A transversal study," *Eur. J. Clin. Microbiol. Infect Dis.*, vol. 36, no. 9, pp. 1559–1563, Sep. 2017.

[19] A. Rumley, "Urine dipstick testing: Comparison of results obtained by visual reading and with the Bayer CLINITEK 50," *Ann. Clin. Biochem.*, vol. 37, no. 2, pp. 220–221, Mar. 2000.

[20] P. Tighe, "Laboratory-based quality assurance programme for near-patient urine dipstick testing, 1990–1997: Development, management and results," *Br. J. Biomed. Sci.*, vol. 56, no. 1, pp. 6–15, 1999.

[21] J. D. Peele, R. H. Gadsden, and R. Crews, "Semi-automated vs. visual reading of urinalysis dipsticks," *Clin. Chem.*, vol. 23, no. 12, pp. 2242–2246, Dec. 1977.

[22] S. Brewster, L. Curtis, and R. Poole, "Urine versus blood ketones," *Pract. Diabetes*, vol. 34, no. 1, pp. 13–15, Jan./Feb. 2017.

[23] R. R. Kalyani, C. D. Saudek, F. L. Brancati, and E. Selvin, "Association of diabetes, comorbidities, and A1C with functional disability in older adults," *Diabetes Care*, vol. 33, no. 5, pp. 1055–1060, May 2010.

[24] J. A. Lott and E. Khabbaza, "Haemoglobin analysis on whole blood by reflectance photometry," *J. Automat. Chem.*, vol. 7, no. 4, pp. 197–200, 1985.

[25] P. Bonini, L. Sanguini, L. Grossi, F. Ceriotti, and M. Murone, "Automation in urinalysis: Evaluation of three urine test strip analysers," *J. Automat. Chem.*, vol. 10, no. 3, pp. 121–129, Jul./Sep. 1988.

[26] M. Ra, M. S. Muhammad, C. Lim, S. Han, C. Jung, and W.-Y. Kim, "Smartphone-based point-of-care urinalysis under variable illumination," *IEEE J. Transl. Eng. Health Med.*, vol. 6, Dec. 2018, Art. no. 2800111.

[27] M. Velikova, R. L. Smeets, J. T. Van. Scheltinga, P. J. F. Lucas, M. Spa, "Smartphone-based analysis of biochemical tests for health monitoring support at home," *Healthcare Technol. Lett.*, vol. 1, no. 3, pp. 92–97, 2014.

[28] J. Hong and B.-Y. Chang, "Development of the smartphone-based colorimetry for multi-analyte sensing arrays," *Lab Chip*, vol. 14, no. 10, pp. 1725–1732, May 2014.

[29] K. Choi *et al.*, "Smartphone-based urine reagent strip test in the emergency department," *Telemed. E-Health*, vol. 22, no. 6, pp. 534–540, May 2016.

[30] H. Yu, Y. Tan, and B. T. Cunningham, "Smartphone fluorescence spectroscopy," *Analyst*, vol. 86, no. 17, pp. 8805–8813, Aug. 2014.

[31] L. Kwon, K. D. Long, Y. Wan, H. Yu, and B. T. Cunningham, "Medical diagnostics with mobile devices: Comparison of intrinsic and extrinsic sensing," *Biotechnol. Adv.*, vol. 34, no. 3, pp. 291–304, May/Jun. 2016.

[32] Y. Qiao *et al.*, "Breath ketone testing: A new biomarker for diagnosis and therapeutic monitoring of diabetic ketosis," *BioMed Res. Int.*, vol. 2014, May 2014, Art. no. 869186. [Online]. Available: https://www.ncbi.nlm.nih.gov/pmc/articles/PMC4037575/ and https://www.hindawi.com/journals/bmri/2014/869186/

Elizabeth V. Woodburn received the B.S. degree in bioengineering from the University of Illinois at Urbana–Champaign in 2018. She is currently pursuing the M.D. degree at the Carle Illinois College of Medicine.

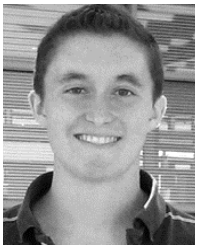

Kenneth D. Long received the B.S. degrees in materials science and engineering and molecular and cellular biology in 2012 and the M.S. and Ph.D. degrees in bioengineering from the University of Illinois at Urbana–Champaign in 2014 and 2018, respectively, where he is currently pursuing the M.D. degree at the College of Medicine.

Brian T. Cunningham (F'12) received the Ph.D. degree from the University of Illinois at Urbana–Champaign in 1990. He joined the Research Division of Raytheon, Lexington, MA, USA, from 1991 to 1995, where he was the Group Leader for the Infrared Sensors Fabrication. He joined the Micromachined Sensors Group, Charles Stark Draper Laboratory, Cambridge, MA, USA, in 1995, as a Senior Member of the Technical Staff, where he later served in management roles that included Group Leader for MEMS Sensors, and the Technical Director for Bioengineering Programs. At Draper Laboratory, he initiated efforts in biosensors, microfluidics, and tissue engineering. In 2000, he became the Founder and the CTO of SRU Biosystems, a company established to commercialize photonic crystal biosensors, detection instruments, and assays for applications in drug discovery and diagnostics. He joined the Faculty of the Department of Electrical and Computer Engineering, University of Illinois at Urbana–Champaign, as an Associate Professor, in 2004, where he established the Nanosensors Group at the Micro and Nanotechnology Laboratory (MNTL). At Illinois, he served as the Director of the NSF-Funded Center for Innovative Instrumentation Technology, the first Industry/University Cooperative Research Center at MNTL, and served among the initial faculty to join the newly formed Bioengineering Department, where he was the Founding Director of the Bioengineering Graduate Program. He established the first M.Eng. professional master's program in bioengineering with strong participation from the UIUC Business School with a specialization in bioinstrumentation. He was appointed as the Interim Director of the MNTL in 2013 and was selected as the Director of MNTL in 2014. He was named as the Donald Biggar Willett Professor of Engineering in 2015.

He has authored or co-authored over 166 peer-reviewed journal papers, over 84 issued U.S. patents, over 133 conference talks, and has delivered over 117 invited lectures. His research interests include biophotonics, bionanophotonics, micro/nanofabrication processes and materials, BioMEMS, lab-on-a-chip, microfluidics, biosensing, and applications in drug discovery, health diagnostics, mobile point-of-use detection systems, life science research, environmental monitoring, animal health, and food safety. His key technical contributions and achievements stem from his invention and the application of nanostructured photonic surfaces that efficiently couple electromagnetic energy into biological analytes, enabling the high signal-to-noise sensing of materials that include small molecules, nucleic acids, proteins, virus particles, cells, and tissues. He has made key foundational contributions to the application of mobile devices (such as smartphones) to point-of-use detection systems that provide equivalent capabilities to laboratory-based instruments. He is a Fellow of AAAS, NAI, OSA, and AIMBE. His work has been recognized through the IEEE Sensors Council Technical Achievement Award in 2010, the IEEE Sensors Council Distinguished Lectureship in 2013, and the Engineering in Medicine and Biology Society Technical Achievement Award in 2014.